

Reduced Order Models Based on Pod Method for Schrödinger Equations

Gerda Jankevičiūtė, Teresė Leonavičienė,
Raimondas Čiegis and Andrej Bugajev

Vilnius Gediminas Technical University

Sauletekio av. 11, Vilnius

E-mail(*corresp.*): gerda.jankeviciute@vgtu.lt

E-mail: terese.leonaviciene@vgtu.lt

E-mail: rc@vgtu.lt

E-mail: andrej.bugajev@vgtu.lt

Received October 15, 2013; revised November 25, 2013; published online December 1, 2013

Abstract. Reduced-order models (ROM) are developed using the proper orthogonal decomposition (POD) for one dimensional linear and nonlinear Schrödinger equations. The main aim of this paper is to study the accuracy and robustness of the ROM approximations. The sensitivity of generated optimal basis functions on various parameters of the algorithms is discussed. Errors between POD approximate solutions and exact problem solutions are calculated. Results of numerical experiments are presented.

Keywords: reduced order model, proper orthogonal decomposition, Schrödinger equation.

AMS Subject Classification: 65L02; 65M02.

1 Introduction

Physical processes described by partial differential equations (PDE's) are usually simulated by discretizing the spatial and the temporal domain of the variables. In this way, numerical approximations of the dynamic behavior of these processes are obtained. As a rule, the finer the discretization, the more accurate the numerical solution of the given PDE are obtained. However, a fine discretization leads to a very large number of equations which need to be solved simultaneously at every time step. Hence, the model complexity increases with increasing requirements on model accuracy. In many problems, specifically when real-time solutions or full stability bifurcation diagrams are required, the need to accelerate the calculations is vital. We note a big progress achieved recently in the acceleration of solution procedures for nonlinear Schrödinger

problems, for example, simplification of the model, high-order accuracy of approximations, parallelization, multigrid iterative solvers, domain decomposition techniques are used to solve these problems faster.

There exist many ways how to derive a simple model from a complex one. Derivation of simple models in general means derivation of models which comprise less number of equations or variables and which are numerically fast for computations or simulations. Such simple models can be derived based on physical insights or based on data collected from simulations or experiments. Hence there are two main approaches for the derivation of simpler models [4]:

- Physical-insight based approach. Using physical insight, an initially complex model can be transformed into a simpler one by considering its physical phenomena.
- Black-box modeling approach. With the advent of system identification techniques, such as subspace identification and neural networks, empirical models can be derived from the input output data.

Model order reduction (MOR) techniques try to reduce the computational complexity and computational time of large scale dynamical systems. The idea is to approximate the given large problem by a problem of much lower dimension that can produce nearly the same response characteristics. Reduced-order modeling is a powerful and ubiquitous tool and it have been given significant attention in recent years. Research in the area of reduced-order modeling has followed two approaches:

- non projection based methods,
- projection based methods.

The vast majority of research is concerned with projection based methods, such as the balanced truncation and POD. There are many papers, where such methods are analyzed and applied for problems in heat transfer [9], fluid mechanics, lithium-ion battery [6], reactor system [13]. The POD method is described in details e.g in [5,17].

A new technique for efficiently solving parametric nonlinear reduced order models in the Proper Generalized Decomposition (PGD) framework is presented in [1]. We also note a new approach to construct efficient reduced-order models for nonlinear PDEs by using the proper orthogonal decomposition combined with the discrete empirical interpolation method, see [7,14]. The algorithm constructs specially selected interpolation indices that specify an interpolation based projection that gives a nearly optimal subspace approximation to the nonlinear term without the expense of orthogonal projection.

The growing interest in the laser technology in many areas of physics, biology and engineering, requires to solve complicated models of quantum mechanics. In the quantum mechanics the basic equation of motion is the Schrödinger equation. The time-dependent Schrödinger equation is a partial differential equation with a form similar to the parabolic heat equation. But this equation describes the motion of the particles by using the wave properties, i.e. the motion of the particle is presented using the wave function.

There exist many efficient numerical methods for solving the Schrödinger equation. They are based on finite-difference schemes (see, e.g., [8, 15, 18]), finite-element and Galerkin approaches (see, [2, 3]), or spectral and pseudo-spectral methods ([19], see also references given therein).

As it is mentioned above, it is important to solve such problems with the low computational costs. In the article [16] (see also references given therein) the POD method is applied for some nonlinear Schrödinger problems, including the simulation of soliton dynamics and the analysis of the sequence of bifurcations that are responsible for the multipulsing instability in the master mode-locking and the waveguide array mode-locking models. The obtained results are proving that the POD method is a very efficient tool for solving such kind of problems. We note that the accuracy of constructed ROMs is directly connected to the fact that the solution space of these problems is embedded into a very low dimensional manifold. Thus it is important to solve examples of linear and nonlinear Schrödinger problems with more general solutions.

In this paper we study the accuracy and robustness of the POD method for solving the linear and nonlinear Schrödinger equations. Our main aim is to investigate the sensitivity of the method with respect to the total number and proper time moments for the selection of data samples. The choice of the snapshot ensemble is one of the most important factors in constructing an accurate POD basis. This choice can greatly affect the approximation of the original solution space.

We also compare two strategies for definition of the orthonormal basis, when data samples are generated in two different regions of the solution. The first one consists in combining both subsets into one big set and the orthonormal POD modes are generated from the obtained SVD. The second approach consists in generation of POD modes for each regime of the solution separately, and the combined set of basis functions is orthogonalized by the Gram–Schmidt algorithm.

The paper is outlined as follows. Section 2 describes the basic procedure for obtaining the POD modes from a given set of data and for derivation of the ROM model by using the Galerkin projection method. Section 3 describes the construction of reduced order models for linear and nonlinear Schrödinger equations. In the Section 4 investigations of the sensitive of the POD method algorithm to the choice of a snapshot ensemble are presented.

2 Reduced Order Models with POD Method

The basic step of most numerical methods is to define a set of basis functions, that are used to construct a numerical approximation of the solution. This set of functions should be a complete set. In addition, for the stability of the algorithm these functions should be linearly independent, an optimal choice is orthonormal functions. Various types of basis functions are selected by different numerical methods: splines, finite elements, sets of trigonometric functions or polynomials are some popular examples.

In the POD method basis functions are generated by using an a priori-information about the solution of PDE, thus the obtained set of functions

is adapted to the specific behaviour of the solution. It is known that this set of basis functions is optimal in some sense. Given a collection of functions $U = \{u_i(x)\}$ on a domain Ω , the goal of the POD process is to produce an optimal orthogonal set of basis functions $\Phi = \{\phi_i(x)\}$ (proper orthogonal modes – POMs) for a space spanned by the given collection.

The following steps describe the POD process, see e.g. [6, 11]. We restrict to the discrete case of functions. First, let us specify the input collection of discrete functions $U \in \mathbb{C}^{N \times K}$:

$$U = [U^1, U^2, \dots, U^K], \quad U^k = (u_1^k, u_2^k, \dots, u_N^k)^T, \quad k = 1, 2, \dots, K, \quad (2.1)$$

where K is the number of samples, N is the number of points per sample.

Second, the singular value decomposition (SVD) of the matrix U is done

$$U = V \Sigma \Psi^*,$$

where $V \in \mathbb{C}^{N \times N}$ is an $N \times N$ complex unitary matrix, $\Psi^* \in \mathbb{C}^{K \times K}$ is a $K \times K$ complex unitary matrix, which is the conjugate transpose of Ψ . The matrix $\Sigma \in \mathbb{C}^{N \times K}$ is an $N \times K$ rectangular diagonal matrix with nonnegative real elements (the singular values of U)

$$\sigma_1 \geq \sigma_2 \geq \dots \geq \sigma_{\tilde{J}} \geq 0, \quad \tilde{J} = \min(K, N).$$

The singular values σ_i and eigenvalues λ_i of UU^* are related by the equation: $\sigma_i^2/K = \lambda_i$. The columns of matrices V and Ψ are called the left-singular and right-singular vectors of matrix U . The left-singular vectors of U are eigenvectors of matrix UU^* .

We select the columns of matrix V as a system of orthonormal basis vectors $\{\Phi^j\}$, $j = 1, \dots, \tilde{J}$. They are called the proper orthogonal modes (POMs).

This system is complete in the sense, that any column of matrix U can be represented as a linear combination of these basis vectors

$$U^k = \sum_{j=1}^{\tilde{J}} \psi_{kj} \sigma_j \Phi^j, \quad k = 1, \dots, K.$$

For most applications the singular values σ_j decay very quickly, therefore it is sufficient to consider a small sized reduced system of basis functions. Thus the ROM is obtained by considering a subspace of functions generated by $M \ll \tilde{J}$ modes, retained in the projection operator

$$P_M U^k = \sum_{j=1}^M c_j^k \Phi^j, \quad k = 1, \dots, K. \quad (2.2)$$

As it follows from the construction of POMs, the POD provides the optimal basis because $P_M U$ is the maximal projection of the initial matrix U onto a linear subspace of the size M [10].

In order to determine the size of the truncated system of basis vectors, let us define the relative energy of the j th mode as

$$E_j = \sigma_j / \sum_{\ell=1}^{\tilde{J}} \sigma_\ell.$$

In all computations of this paper, the truncated basis is selected as a minimal number of modes with energies that sum to $\sum_{j=1}^M E_j \geq 0.9999$ of the total energy.

Next we present a general template of the POD method for solving some nonstationary PDE.

- Compute the basis functions as the first POMs Φ^k , $k = 1, \dots, M$.
- Construct the approximation of the exact solution as a linear decomposition

$$\tilde{U}^k(x_n) = \sum_{j=1}^M c_j(t^k) \Phi^j(x_n), \quad k = 1, \dots, K, \quad n = 1, \dots, N, \quad (2.3)$$

where x_n is a point of the discrete space grid, and t^k is a point of the discrete time grid.

- Substitute the approximation (2.3) of the state variables into the discrete model (some finite difference, finite element or finite volume scheme), and project the resulting system onto the low order subspace of M modes to obtain the reduced order model (ROM).
- Solve the obtained ROM for the reduced variables. Reconstruct the original discrete field variables.

3 POD Method for Schrödinger Problems

In this section we construct reduced order models for linear and nonlinear one-dimensional Schrödinger problems.

3.1 Linear Schrödinger equation

We consider the linear Schrödinger equation:

$$\begin{cases} i \frac{\partial u}{\partial t} + D_f \frac{\partial^2 u}{\partial x^2} = 0, & x_L \leq x \leq x_R, \quad t > 0, \quad i = \sqrt{-1}, \\ u(x_L, t) = 0, \quad u(x_R, t) = 0, & 0 < t \leq T, \\ u(x, 0) = u_0(x), & x_L \leq x \leq x_R, \end{cases} \quad (3.1)$$

where $u = u(x, t)$ is a complex-valued function of two real variables x, t , D_f is a real constant. We define a uniform grid: $\omega_h = \omega_{h_x} \times \omega_{h_t}$:

$$\begin{aligned} \omega_{h_x} &= \{x_j: x_j = jh_x, \quad j = 0, 1, \dots, N, \quad x_0 = x_L, \quad x_N = x_R\}, \\ \omega_{h_t} &= \{t^k: t^k = kh_t, \quad k = 0, 1, \dots, \tilde{K}, \quad \tilde{K}h_t = T\}. \end{aligned}$$

Let u_j^k be a discrete function, which approximates the exact solution $u(x_j, t^k)$ of the given differential problem.

We define the following discrete operators:

$$(u_j^k)_x = \frac{u_{j+1}^k - u_j^k}{h_x}, \quad (u_j^k)_{\bar{x}} = \frac{u_j^k - u_{j-1}^k}{h_x}, \quad (u_j^k)_t = \frac{u_j^{k+1} - u_j^k}{h_t}. \quad (3.2)$$

By using the finite-difference method we approximate (3.1) by the classical Crank–Nicolson scheme [15, 18]:

$$\begin{aligned} iu_t + D_f \left(\frac{u^{k+1} + u^k}{2} \right)_{\bar{x}x} &= 0, \\ u_0^k &= 0, \quad u_N^k = 0, \quad k = 1, \dots, \tilde{K}, \\ u_j^0 &= u_0(x_j), \quad j = 0, \dots, N. \end{aligned} \quad (3.3)$$

It is well-known, that this scheme is unconditionally stable and the error estimate of order $\mathcal{O}(h_t^2 + h_x^2)$ is valid [8, 15].

We write equation (3.3) in the matrix form

$$i(U^{k+1} - U^k) + AU^{k+1} + AU^k = 0, \quad (3.4)$$

where the vector $U^k = (u_1^k, \dots, u_{N-1}^k)^T$, and A is the following $(N - 1) \times (N - 1)$ matrix

$$A = \begin{bmatrix} \frac{h_t D_f}{h_x^2} & \frac{-h_t D_f}{2h_x^2} & 0 & 0 & \dots & 0 \\ \frac{-h_t D_f}{2h_x^2} & \frac{h_t D_f}{h_x^2} & \frac{-h_t D_f}{2h_x^2} & 0 & \dots & 0 \\ \dots & \dots & \dots & \dots & \dots & \dots \\ 0 & \dots & 0 & 0 & \frac{-h_t D_f}{2h_x^2} & \frac{h_t D_f}{h_x^2} \end{bmatrix}. \quad (3.5)$$

The dynamics of the discrete solution U^k is simulated by using the M mode expansion

$$\tilde{U}^k = \sum_{j=1}^M c_j^k \Phi^j, \quad (3.6)$$

where Φ^j are the POD modes obtained by using the solution of discrete problem (3.3) and coefficients c_j^k are the reduced variables. Substituting this linear combination into equation (3.4) yields the following equation

$$\sum_{j=1}^M [i(c_j^{k+1} - c_j^k) \Phi^j + (c_j^{k+1} + c_j^k) A \Phi^j] = 0.$$

The inner product is taken with respect to Φ^ℓ , which gives the reduced order model

$$\begin{aligned} i(c_\ell^{k+1} - c_\ell^k) + \sum_{j=1}^M (c_j^{k+1} + c_j^k) (A \Phi^j, \Phi^\ell) &= 0, \quad \ell = 1, \dots, M, \\ c_\ell^0 &= (U^0, \Phi^\ell). \end{aligned} \quad (3.7)$$

Coefficients $(A\Phi^j, \Phi^\ell)$ are precomputed only once, thus the complexity of the obtained reduced order model depends only on M , but not on total number of grid points N . At each time level the obtained system of linear equations is solved by using the standard Gauss method, thus the complexity of the POD algorithm is $\mathcal{O}(KM^3)$.

The error between ROM solution \tilde{U}^k and the exact solution $u(x, t^k)$ of the differential problem can be estimated as [11]

$$|\tilde{U}_j^k - u(x_j, t^k)| = \mathcal{O}(\max\{\sigma_{M+1}e^{\tilde{K}/K}, h_t^2, h_x^2\}), \quad (3.8)$$

σ_{M+1} is the first rejected singular value, \tilde{K} is the number of time steps, K is the number of snapshots (the number of solutions which are used to extract POMs).

3.2 Nonlinear Schrödinger equation

In this section we consider the cubic nonlinear Schrödinger (NLS) equation:

$$\begin{cases} i \frac{\partial u}{\partial t} + D_f \frac{\partial^2 u}{\partial x^2} + q|u|^2u = 0, & x_L \leq x \leq x_R, t > 0, i = \sqrt{-1}, \\ u(x_L, t) = 0, \quad u(x_R, t) = 0, & 0 < t \leq T, \\ u(x, 0) = u_0(x), & x_L \leq x \leq x_R, \end{cases} \quad (3.9)$$

where q is a non-zero real parameter. Such models of the NLS equation (3.9) and various generalizations occur in various areas of physics such as nonlinear optics, water waves, plasma physics, quantum mechanics, superconductivity and Bose–Einstein condensate theory. In optics, the NLS equation models many nonlinearity effects in a fiber, including but not limited to self-phase modulation, four-wave mixing, second harmonic generation, stimulated Raman scattering, etc. For water waves, the NLS equation describes the evolution of the envelope of modulated nonlinear wave groups.

We approximate NLS equation (3.9) by the following Crank-Nicolson scheme:

$$iu_t + D_f \left(\frac{u^{k+1} + u^k}{2} \right)_{\bar{x}x} + q \frac{(|u^{k+1}|^2 + |u^k|^2)}{2} \frac{(u^{k+1} + u^k)}{2} = 0. \quad (3.10)$$

The stability and convergence rate $\mathcal{O}(h_t^2 + h_x^2)$ of the discrete algorithm is proved in many papers, see [15, 18].

The discrete problem (3.10) can be written in the operator form:

$$i(U^{k+1} - U^k) + AU^{k+1} + AU^k + \frac{qh_t}{4} (|U^{k+1}|^2 + |U^k|^2)(U^{k+1} + U^k) = 0, \quad (3.11)$$

where $U^k = (u_1^k, \dots, u_{N-1}^k)^T$ and matrix A is defined in (3.5). Substituting the linear combination (3.6) of POD modes into equation (3.11) and computing the inner product with respect to Φ^ℓ , we obtain the nonlinear reduced order model

$$\begin{aligned} & \left(i(\tilde{U}^{k+1} - \tilde{U}^k) + A\tilde{U}^{k+1} + A\tilde{U}^k + \frac{qh_t}{4} (|\tilde{U}^{k+1}|^2 + |\tilde{U}^k|^2)\tilde{U}^{k+1} \right. \\ & \left. + \frac{qh_t}{4} (|\tilde{U}^{k+1}|^2 + |\tilde{U}^k|^2)\tilde{U}^k, \Phi^\ell \right) = 0, \quad \ell = 1, \dots, M. \end{aligned}$$

The derived nonlinear problem is solved by applying the following simple iterative linearization technique, see also [20]:

$$\begin{aligned} & i(\tilde{c}_\ell^s - \tilde{c}_\ell^k) + \sum_{j=1}^M (\tilde{c}_j^s + \tilde{c}_j^k)(A\Phi^j, \Phi^\ell) \\ & + \frac{qh_t}{4} ((|\tilde{U}^{s-1}|^2 + |\tilde{U}^k|^2)(\tilde{U}^{s-1} + \tilde{U}^k), \Phi^\ell) = 0, \quad \ell = 1, \dots, M. \end{aligned} \tag{3.12}$$

We begin from an initial condition $\tilde{U} = \tilde{U}^k$ and conduct iterations until convergence, when the following criterion is satisfied:

$$\max_j |\tilde{U}_j^s - \tilde{U}_j^{s-1}| \leq 10^{-8} \max_j |\tilde{U}_j^s|.$$

The direct implementation of the reduced order model (3.12) computationally is not efficient, see [7]. In order to compute the nonlinear term, values of linear combination (3.6) must be computed at any iteration s . It requires NM flops, therefore the algorithm has a computational complexity that depends on N , the dimension of the original full-order system. As was noted above, a new approach is proposed to construct efficient reduced-order models for nonlinear PDEs by using the proper orthogonal decomposition combined with the discrete empirical interpolation method, see [7, 14].

For cubic nonlinearity it is possible to precompute coefficients

$$(\Phi^j \Phi^{*k} \Phi^n, \Phi^\ell), \quad 1 \leq j, k, n, \ell \leq M.$$

Then the computational complexity of the reduced order model does not depend on N . Such an implementation of the POD algorithm is efficient if M is small.

4 Numerical Experiments

In this section we present results of numerical experiments. Our main aim is to investigate the sensitivity of the POD algorithm to the choice of a snapshot ensemble. The goal is to present some simple rules and heuristics helping the user in constructing an accurate POD basis.

In our experiments we will use a special algorithm to select the snapshot ensemble. Let assume that we have a set of data examples (snapshots) $D = \{V^1, \dots, V^P\}$. Then Algorithm 1 defines a snapshot ensemble $S = \{U^1, \dots, U^K\}$, $K \leq P$, which is used to construct a POD basis. Here \tilde{S} denotes a set of all elements

$$\tilde{S} = \left\{ U: U = \sum_{j=1}^K c_j U^j \right\},$$

where c_j are any real numbers. The main idea of this algorithm is at each step to add a new snapshot which is most distant from the linear subspace generated by all selected snapshots. The function $\rho(V, \tilde{S})$ measures this distance.

Algorithm 1 Selection of the snapshot ensemble

- 1: select $U^1 = V^j$;
 - 2: initialize $k = 1$, $S = \{U^1\}$, $D = D \setminus \{U^1\}$;
 - 3: **while** ($k < K$) **do**
 - 4: $k = k + 1$;
 - 5: find $U^k = \arg \max_{V \in D} \rho(V, \tilde{S})$;
 - 6: update $S = S \cup \{U^k\}$, $D = D \setminus \{U^k\}$;
 - 7: **end while**
-

Next we consider a case when a solution of the given PDE defines a traveling wave (or soliton) which moves with a constant velocity. Then we can use the following distance function

$$\rho(V^k, \tilde{S}) = \min_{V^j \in \tilde{S}} |k - j|. \quad (4.1)$$

This algorithm generates the set of snapshots in blocks. First, the data is taken on a coarse time grid $\{t^0 = 0, t^1 = TF/2, t^2 = TF\}$. At the second step the additional snapshots are taken on the time grid $h_t = TF/4$ and this process is continued iteratively.

The Algorithm 1 is stopped when the number of selected POMs is not changing in two consequent steps.

4.1 Linear problem

In this section we investigate the POD method for the linear Schrödinger equation (3.1).

We consider the case when $D_f = 1/2$ and the exact solution of this problem is defined by

$$u(x, t) = \sqrt{\frac{i}{-2t + i}} \exp\left(\frac{ix^2 + vx - gt}{2t - i}\right).$$

Problem (3.1) is solved in the interval $[-10, 50]$ for traveling Gaussian wave when $v = 4$, $g = 8$, the final time $T = 6.4$. We note that about 150 Fourier modes are required to obtain the accurate approximation of the exact solution.

First, we have investigated the dependence of POD basis on the selection of snapshots. The snapshots are generated by using the exact solution with uniform time steps T/\tilde{K} and sufficiently small space step, such that the accuracy of basis functions is not depending on space mesh. Then a solution of the reduced order model (3.7) is computed. The following uniform meshes were used to solve the reduced order model: $h_x = 0.05$, $h_t = 0.01$. Figure 1 demonstrates the distribution of singular values σ_j on log scale.

In Table 1 we list the number of POMs M and the error ε of the approximate solution for various numbers of uniformly distributed snapshots K . The error

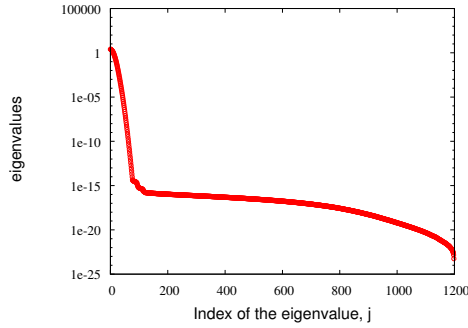


Figure 1. Singular values σ_j of the linear Schrödinger equation (3.1) for a travelling wave solution

Table 1. Numerical results for linear problem (3.1) at time $T = 6.4$: a uniform distribution of snapshots.

K	11	21	41	81	161	321	641
ϵ	0.79847	0.23995	0.02501	0.02305	0.02295	0.02281	0.02269
M	10	20	37	38	38	38	38

ϵ is computed as

$$\epsilon = \max_{0 \leq k \leq \tilde{K}} \left(\max_{0 \leq j \leq N} |\tilde{U}_j^k - u(x_j, t^k)| \right),$$

where \tilde{U}_j^k is a solution of the reduced order model.

The results listed in Table 1 show that $K = 81$ snapshots are sufficient to construct an accurate POD basis and the number of POD modes is essentially smaller than the number Fourier modes required to approximate the same travelling wave solution with the given accuracy.

Next we have investigated the assumption that for travelling wave solutions the accuracy of POD basis set depends on the maximum time step among two neighbour snapshots. A uniform set of snapshots S_{81} with $K = 81$ is used as a starting set, and some particular cases of data $S = \{U^\ell, \ell = 1, \dots, L\}$ are excluded from this set. The results are listed in Table 2, where

$$\begin{aligned} S^1 &= \{U^{42}\}, & S^2 &= \{U^{42}, U^{48}\}, & S^3 &= \{U^{40}, U^{41}, U^{42}, U^{48}\}, \\ S^4 &= \{U^{39}, U^{40}, U^{41}, U^{42}, U^{48}\}, & S^5 &= \{U^{36}, U^{37}, U^{38}, U^{40}, U^{41}, U^{42}\}. \end{aligned}$$

The presented results show that the accuracy of POD approximations depends on the time step among two neighbor snapshots in some integral norm, which is still close to the maximum norm.

Similar conclusions can be done from results of computational experiments when time moments of snapshots are distributed in random in the interval $[0, T]$. The results are listed in Table 3, where d denotes the maximum distance between neighbor snapshots.

Table 2. Numerical results for linear problem (3.1) at time $T = 6.4$: snapshots S^ℓ are excluded from the set of uniformly distributed snapshots S_{81} .

$S_{81} \setminus S$	S^1	S^2	S^3	S^4	S^5
ε	0.0230	0.0230	0.0230	0.02707	0.03619
M	38	38	38	38	38

Table 3. Numerical results for linear problem (3.1) at time $T = 6.4$: a non-uniform distribution of snapshots.

K	11	21	41	81	161	321	641
ε	0.6586	0.16366	0.02897	0.02915	0.02891	0.02886	0.02882
M	10	20	36	38	38	38	38
d	0.75142	0.38106	0.20306	0.11079	0.06361	0.03879	0.01983

Table 4. Numerical results for linear problem (3.1) at time $T = 6.4$: the complete basis set is obtained by combining dominating POD modes in each subdomain.

\widetilde{M}	2	3	4	5
	[0, 2.5](2.5, 6.4]	[0, 2.5](2.5, 3.5] (3.5, 6.4]	[0, 1.25](1.25, 2.5] (2.5, 3.75](3.75, 6.4]	[0, 1](1, 2](2, 3] (3, 4](4, 5](5, 6.4]
ε	0.02188	0.02163	0.02143	0.02159
M	21 + 21	15 + 15 + 15	10 + 10 + 10 + 17	8 + 8 + 8 + 8 + 16

The presented results and results given in Table 1 are very similar if d is related to the time step T/\widetilde{K} .

The union of the POD modes from different regions. An interesting modification of the classical POD method is obtained if the reduced order model is derived by using the dominating modes from different regions. The full set of POD modes is constructed by combining all subsets into one set of basic POD modes. For example this approach was applied in [16], where the multipulsing transition of the cubic-quintic Ginzburg–Landau problem was investigated.

We have constructed reduced order models, when the interval $[0, T]$ is covered by non-overlapping subintervals, and dominating POD modes are computed in each subdomain. Then the obtained modes are combined into one set. The combined basis functions are orthogonalized by the Gram–Schmidt algorithm. The results are listed in Table 4, where \widetilde{M} denotes the number of subintervals in the decomposition of the full time interval

$$[0, 6.4] = [t_s^1, t_f^1] \cup \dots \cup (t_s^{\widetilde{M}}, t_f^{\widetilde{M}}].$$

It follows from the presented results that the combined basis set of POD modes preserves the global accuracy of the reduced order model. The size of the obtained basis set is increased for the increased number of subintervals, thus redundant modes are included into the combined basis set.

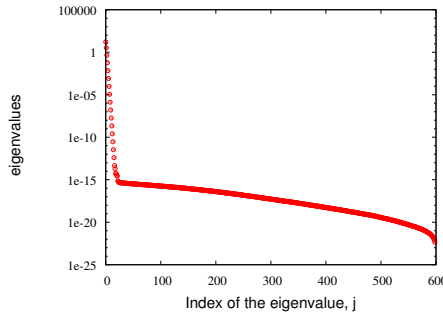


Figure 2. Singular values σ_j of the nonlinear Schrödinger equation (3.9) for a traveling soliton solution

Table 5. Numerical results for nonlinear problem (3.9): a uniform distribution of snapshots, traveling soliton $\alpha = 0.5$.

K	11	21	41	81	161	321	641
ε	0.00693	0.00631	0.00675	0.00709	0.007279	0.00737	0.00742
M	6	6	6	6	6	6	6

4.2 Nonlinear problem

In this section we investigate the POD method for the nonlinear Schrödinger (NLS) equation (3.9). It is well known that the NLS equation with $D_f = 1$ admits various soliton solutions, here we consider the soliton [12]:

$$u(x, t) = k \sqrt{\frac{2}{q}} \operatorname{sech}(k(x - 2\alpha t)) e^{i(\alpha x - (\alpha^2 - k^2)t)}, \tag{4.2}$$

where α, k are arbitrary real constants, and $q > 0$ for the self-focusing case. Let the problem is defined in the interval $x \in [-10, 20]$, and parameters $q = 2, k = 0.5, \alpha = 0.5$ are used.

The snapshots are generated by using the exact solution with uniform time steps T/\tilde{K} with $T = 6.4$ and sufficiently small space step. Then a solution of the reduced order model (3.12) is computed. Figure 2 demonstrates the distribution of singular values σ_j on log scale.

In Table 5 we list the number of POMs M and the error ε of the approximate solution for various numbers of uniformly distributed snapshots K .

The results listed in Table 5 show that $K \approx 15$ snapshots are sufficient to construct an accurate POD basis, and the size of the POD basis set $M = 6$ is very small. Thus the reduced order model (3.12) can be implemented very efficiently by using the precomputed coefficients for the nonlinear interaction term. A similar result is obtained in [16] for the case of standing $N \operatorname{sech}(x)$ type solitons, when it is sufficient to use one or two dominant POD modes.

Next we have extended this analysis for the case, when the velocity of a soliton is increased. In Table 6 we list the number of POMs M and the error ε of the approximate solution for various numbers of uniformly distributed

Table 6. Numerical results for nonlinear problem (3.9): a uniform distribution of snapshots, traveling soliton $\alpha = 1$.

K	11	21	41	81	161	321	641
ε	0.10195	0.00698	0.00467	0.00438	0.00468	0.00494	0.00508
M	11	18	18	18	18	18	18

snapshots K , when $\alpha = 1$. The problem is solved in the domain $[-10, 30] \times (0, 12.8]$. The remaining parameters are the same as in previous experiments.

From the given results we see that the number of required modes M is increased, when the soliton is moving faster. These results agree well with conclusions done in the case of a traveling wave for a linear problem.

Acknowledgement

The work was supported by Eureka project E!6799 POWEROPT “Mathematical modelling and optimization of electrical power cables for an improvement of their design rules”.

References

- [1] J.V. Aguado, F. Chinesta, A. Leygue, E. Cueto and A. Huerta. DEIM – based PGD for parametric nonlinear order reduction. In J.P. Moitinho de Almeida, P. Deze, C. Tiago and N. Pares(Eds.), *VI International Conference on Adaptive Modeling and Simulation, ADMOS 2013*, pp. 29–37, Barcelona, Spain, 2013. International Center for Numerical Methods in Engineering (CIMNE).
- [2] G.D. Akrivis, V.D. Dougalis and V.A. Karakashian. On fully discrete Galerkin methods of second-order temporal accuracy for the nonlinear Schrödinger equation. *Numer. Math.*, **59**:31–53, 1991.
- [3] X. Antoine, A. Arnold, Ch. Besse, M. Ehrhardt and A. Schädle. A review of transparent and artificial boundary conditions techniques for linear and nonlinear Schrödinger equations. *Commun. Comput. Phys.*, **4**(4):729–796, 2008.
- [4] P. Astrid. *Reduction of process simulation models: a proper orthogonal decomposition approach*. PhD thesis, Technische Universiteit Eindhoven, Eindhoven, 2004.
- [5] G. Berkooz, P. Holmes and J.L. Lumley. The proper orthogonal decomposition in the analysis of turbulent flows. *Annu. Rev. Fluid Mech.*, **25**:539–575, 1993. <http://dx.doi.org/10.1146/annurev.fl.25.010193.002543>.
- [6] L. Cai and R.E. White. Reduction of model order based on proper orthogonal decomposition for lithium-ion battery simulations. *J. Electrochemical Soc.*, **156**(3):A154–A161, 2009. <http://dx.doi.org/10.1149/1.3049347>.
- [7] S. Chaturantabut and D.C. Sorensen. Nonlinear model reduction via discrete empirical interpolation. *SIAM J. Sci. Comput.*, **32**(5):2737–2764, 2010. <http://dx.doi.org/10.1137/090766498>.
- [8] R. Čiegis, I. Laukaitytė and M. Radziunas. Numerical algorithms for Schrödinger equations with artificial boundary conditions. *Numer. Funct. Anal. Optim.*, **30**(9-10):903–923, 2009. <http://dx.doi.org/10.1080/01630560903393097>.

- [9] A. Fic, R.A. Bialecki and A.J. Kassab. Solving transient nonlinear heat conduction problems by proper orthogonal decomposition and the finite element method. *Numerical Heat Transfer, Part B*, **48**:103–124, 2005. <http://dx.doi.org/10.1080/10407790590935920>.
- [10] G. Kerschen, J.C. Golinval, A.F. Vakakis and L.A. Bergman. The method of proper orthogonal decomposition for dynamical characterization and order reduction of mechanical systems: an overview. *Nonlinear Dynam.*, **41**:147–169, 2005. <http://dx.doi.org/10.1007/s11071-005-2803-2>.
- [11] K. Kunisch and S. Volkwein. Galerkin proper orthogonal decomposition methods for a general equation in fluid dynamics. *SIAM J. Numer. Anal.*, **40**(2):492–515, 2002. <http://dx.doi.org/10.1137/S0036142900382612>.
- [12] W.X. Ma and M. Chen. Direct search for exact solution to the nonlinear Schrödinger equation. *Appl. Math. Comput.*, **215**:2835–2842, 2009. <http://dx.doi.org/10.1016/j.amc.2009.09.024>.
- [13] A. Marquez, J. Espinosa Oviedo and D. Odloak. Model reduction using proper orthogonal decomposition and predictive control of distributed reactor system. *J. Control Sci. Eng.*, 2013. <http://dx.doi.org/10.1155/2013/763165>.
- [14] B. Peherstorfer, D. Butnaru, K. Willcox and H.-J. Bungartz. Localized discrete empirical interpolation method. Technical Report TR-13-1, MIT Aerospace Computational Design Laboratory, June 2013.
- [15] J.M. Sanz-Serna and J.G. Verwer. Conservative and non-conservative schemes for the solution of the nonlinear Schrödinger equation. *IMA J. Numer. Anal.*, **6**(1):25–42, 1986. <http://dx.doi.org/10.1093/imanum/6.1.25>.
- [16] E. Shlizerman, E. Ding, M.O. Williams and J. Nathan Kutz. The proper orthogonal decomposition for dimensionality reduction in mode-locked lasers and optical systems. *Int. J. Optics*, **2012**:18, 2012. <http://dx.doi.org/10.1155/2012/831604>. Article ID 831604
- [17] P. Sun, Z. Luo and Y. Zhou. Some reduced finite difference schemes based on a proper orthogonal decomposition technique for parabolic equations. *Appl. Numer. Math.*, **60**:154–164, 2010. <http://dx.doi.org/10.1016/j.apnum.2009.10.008>.
- [18] T.R. Taha and M.J. Ablowitz. Analytical and numerical aspects of certain nonlinear evolution equations. II. Numerical Schrödinger equation. *J. Comp. Phys.*, **55**:203–230, 1994. [http://dx.doi.org/10.1016/0021-9991\(84\)90003-2](http://dx.doi.org/10.1016/0021-9991(84)90003-2).
- [19] M. Thalhammer, M. Caliari and Ch. Neuhauser. High-order time-splitting Hermite and Fourier spectral methods. *J. Comput. Phys.*, **228**:822–832, 2009. <http://dx.doi.org/10.1016/j.jcp.2008.10.008>.
- [20] M.D. Todorov and C.I. Christov. Conservative numerical scheme in complex arithmetic for coupled nonlinear Schrödinger equations. *Discrete Contin. Dyn. Syst. Suppl.*, pp. 982–S992, 2007.